Available online at www.sciencedirect.com

ScienceDirect

Mendeleev Commun., 2017, **27**, 592–594

Mendeleev Communications

Complex tunnel structure of new $La_6(Mo_2O_7)(MoO_4)_8$: crystal growth from flux and high structural complexity

Marie Colmont,* Bastien Leclercq, Olivier Mentré and Pascal Roussel

Université Lille Nord de France, Unité de Catalyse et de Chimie du Solide (UCCS–CNRS UMR8181), ENSCL–USTL, 59652 Villeneuve d'Ascq, France. E-mail: marie.colmont@ensc-lille.fr

DOI: 10.1016/j.mencom.2017.11.018

The new lanthanum molybdenum oxide $La_6(Mo_2O_7)(MoO_4)_8$ was synthesized using a flux growth technique, and its crystal structure was determined by single crystal X-ray diffraction analysis.

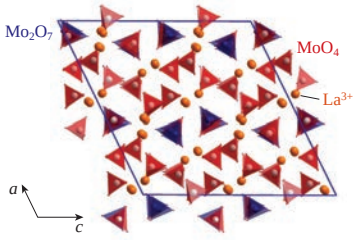

A large number of theoretical and experimental studies were devoted to the La_2O_3–MoO_3 binary system after the evidence of large anionic conductivity in $La_2Mo_2O_9$ derivatives at the origin of the LAMOX (LAnthanum MOlybdenum OXides) series involving compounds with high ionic conductivity performances.[1] Substitution for lanthanum,[2] molybdenum[3] and oxygen[4] in these materials was studied. In the parent chemical system with distinct structural architectures, 22 compounds have been reported; however, none of them gave so interesting properties as those of the above $La_2Mo_2O_9$[1] due to a phase transition into oxygen disordered polytypes. Standard solid-solid routes have been intensively used, and only alternative methods like out-of-equilibrium flux growth techniques and high-pressure conditions may lead to the discovery of new terms. We selected a flux growth technique for its capacity to stabilize novel complex compounds. Here, we present a new lanthanum molybdate isolated by serendipity. Indeed, high-temperature solubility in flux assorted with further precipitations is recognized as a method of choice to grow the single crystals of unexpected inorganic materials.[5] The choice of the flux itself is of crucial importance for the solubilization of the O^{2-} templating anion and the control of the metal redox. Various fluxes of oxides, halides or hydroxides are mainly used for this prospection.[6] For the current case, MoO_3 was used as a solvent for crystallization (i) due to its relatively low melting point (795 °C) and (ii) because Mo would play a tandem role as a flux and phase formatting cation.

Here, we report the synthesis and structural characterization of $La_6(Mo_2O_7)(MoO_4)_8$ and discuss its structural relations to an isoformular phase of $Ce_6(Mo_2O_7)(MoO_4)_8$.[7]

The colorless block-shaped single crystals of $La_6(Mo_2O_7)(MoO_4)_8$ were grown from a molten molybdenum oxide flux.†

The structure of $La_6(Mo_2O_7)(MoO_4)_8$ was studied by single-crystal X-ray diffraction analysis.‡ To check the presence of iron in reaction products, semiquantitative EDX analysis was performed on the single crystal used for the structure solution, confirming the absence of iron from the selected crystals, while the determined La : Mo ratio was 6.2 : 9.9 in good agreement with the title stoichiometry. The crystal structure was undoubtedly refined in the NCS space group *Cc* due to the positions of La atoms. The Flack and $|E^2 - 1|$ parameters were refined to 0.47(5) and 1.091. The refined structure of $La_6(Mo_2O_7)(MoO_4)_8$ is presented in Figure 1(*a*). Although it is isoformular with $Ce_6(Mo_2O_7)(MoO_4)_8$,[7] these two crystal structures do not coincide. Selected structural data for $La_6(Mo_2O_7)(MoO_4)_8$ and $Ce_6(Mo_2O_7)(MoO_4)_8$ are given in Table 1.

The crystal structure of $La_6(Mo_2O_7)(MoO_4)_8$ contains 12 crystallographically independent La sites with VIII [La(1)–(5),(7),(8),(11),(12)] or IX [La(6),(9),(10)] oxygen coordinations and La–O distances varying between 2.3690 and 2.8349 Å. We found not less than 20 independent Mo sites respectively involved, for sixteen of them, in orthomolybdate MoO_4 tetrahedra (with typical molybdate Mo–O bond distances between 1.69 and 1.81 Å) and four, in pyromolybdate Mo_2O_7 corner-sharing pairs of tetrahedra [*i.e.*, Mo(6)/(14) and Mo(10)/(11) pairs]. As expected, the molybdenum–oxygen distances are similar (1.70–1.90 Å), apart the longest distances [Mo(10)–O(56), Mo(11)–O(56),

† Typically, a mixture of $La(OH)_3$, MoO_3 and Fe_2O_3 was taken in the molar ratio 3 : 15 : 0.5. This mixture was loaded into a gold tube, sealed and then heated at 900 °C for 48 h and finally cooled to room temperature for 20 h (cooling rate, 40 K h^{-1}). Finally, the furnace was switched off, and reddish crystals were handily selected under a 60× Nikon binocular.

‡ *Single crystal XRD analysis*. A single crystal of the compound was collected using a Bruker X8 APEX II CCD diffractometer [λ(MoKα) = = 0.71073 Å]. The intensity data were extracted from the collected frames using SAINT-Plus 8.27b.[8] The unit cell parameters were refined from the complete data set. Absorption corrections were performed by multi-scan methods using SADABS.[9] The crystal structure was solved using SUPERFLIP[10] involving the recent charge flipping method and the data were refined with the JANA2006[11] crystallographic suite. After absorption correction, 12209 reflections [$I > 3\sigma(I)$] were merged in the Laue space group 2/*m* leading to the merging factor R_{int} = 0.0596 for 8533 reflections with $I > 3\sigma(I)$. The refined monoclinic lattice parameters of $La_6Mo_{10}O_{39}$ are a = 23.0800(8), b = 14.7146(5) and c = 23.0257(7) Å, β = 116.54(1)°. The complete analysis of the data set revealed that the systematic absences were consistent with the monoclinic NCS space group *Cc*. For details, see Online Supplementary Materials.

CSD 432600 contains the supplementary crystallographic data for this paper. These data can be obtained from FIZ Karlsruhe, 76344 Eggenstein-Leopoldshafen, Germany, http://www.fiz-karlsruhe.de/.

Table 1 Crystallographic data for $La_6(Mo_2O_7)(MoO_4)_8$, $Ce_6(Mo_2O_7)(MoO_4)_8$[7] and $Eu_6(Mo_2O_7)(MoO_4)_8$.[13]

Structure	Space group	a/Å	b/Å	c/Å	α/deg	β/deg	γ/deg	V/Å^3	d_{calc}/g cm^{-3}	Z
$La_6(Mo_2O_7)(MoO_4)_8$	Cc	23.0800(8)	14.7146(5)	23.0257(7)	90.00	116.54(1)	90.00	6996.1(4)	4.11	8
$Ce_6(Mo_2O_7)(MoO_4)_8$	$P\bar{1}$	10.148(5)	18.764(6)	9.566(5)	103.12(7)	78.07(7)	107.69(7)	1671.37	4.82	2
$Eu_6(Mo_2O_7)(MoO_4)_8$	$C2/c$	12.425(1)	19.860(2)	13.882(1)	90.00	100.767(2)	90.00	3365.22	5.07	4

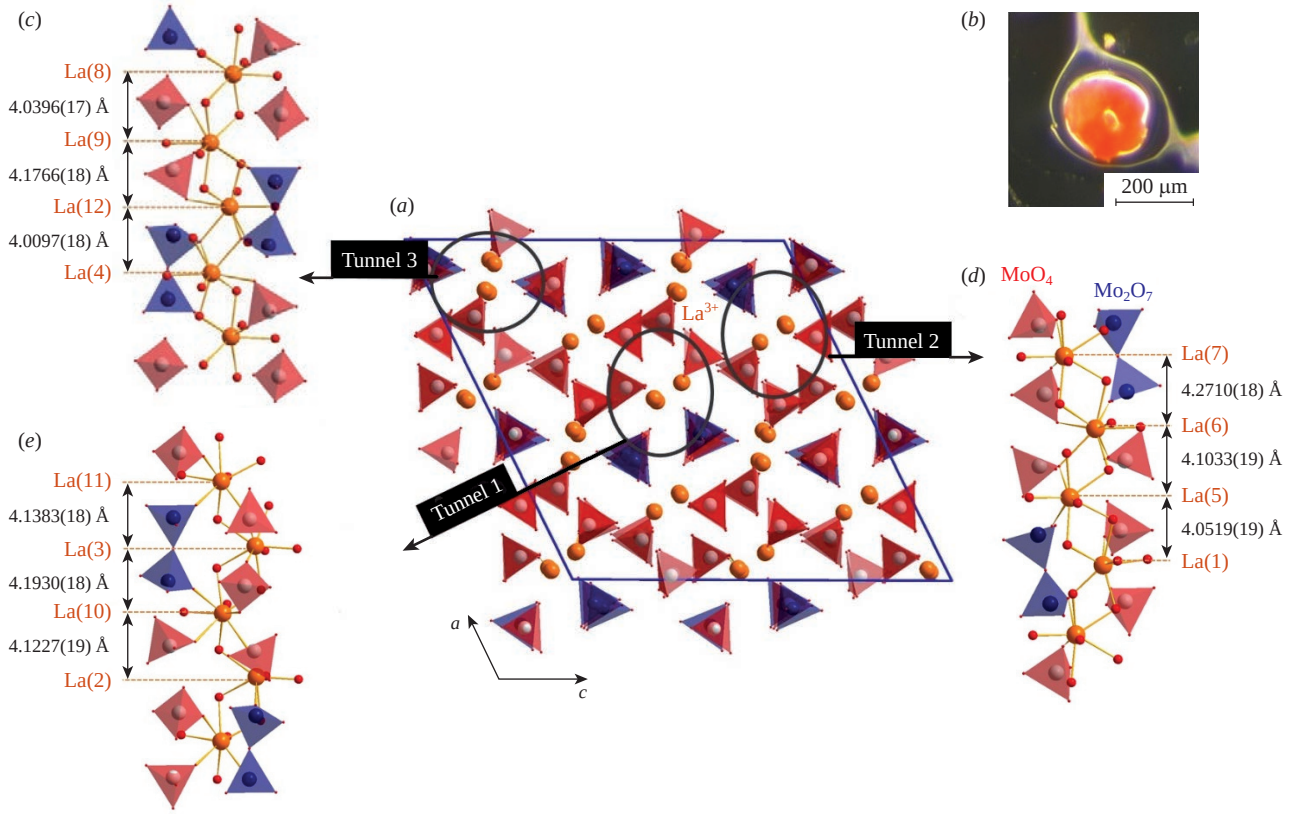

Figure 1 (*a*) Projection along *b* axis of the new $La_6(Mo_2O_7)(MoO_4)_8$, (*b*) crystal observed by optical microscopy and (*c*)–(*e*) surrounding La^{3+} guests with their oxygen neighbours highlighted in three different tunnels.

Mo(6)–O(22) and Mo(14)–O(22)] along the Mo–O–Mo bridges. The MoO_4 and Mo_2O_7 units are arranged three-dimensionally to create three different tunnel types labeled tunnels 1, 2 and 3 in Figure 1, in which the La atoms are hosted. The three tunnels are running along the *b* axis, and appear to be of a circular shape with similar *ac* cross sections. Each tunnel hosts 4 independent lanthanum atoms, along *b* axis, distant from each other from 4.01 to 4.27 Å. The complexity of the crystal structure, especially along this direction, is driven by the ortho- and pyromolybdate groups disposed in the absence of any symmetric relation within each individual tunnel and responsible for the large *b* parameter [14.7146(5) Å].

Compound $Ce_6(Mo_2O_7)(MoO_4)_8$ crystallizes in a triclinic unit cell (see Table 1) with 6 La, 10 Mo and 39 O sites. Like $La_6(Mo_2O_7)(MoO_4)_8$, it includes MoO_4 tetrahedra and Mo_2O_7 pyromolybdates forming tunnels hosting Ce atoms. The Mo–O and Ce–O distances stand in the same range as compared to the above for the La-based compound. However, in the Ce compound, we count four individual tunnels, and three of them are similarly shaped to that of the La compound (Figure 2, tunnels 1–3) while tunnel 4 displays an elongated section. It is built on an association of two adjacent tunnels with opening the middle wall. The length of the so-created cavity is almost twice the distance of a tunnel diameter in $La_6(Mo_2O_7)(MoO_4)_8$. This is the main difference between the two structures. Furthermore, the orientation of MoO_4 and Mo_2O_7 is more misaligned in the Ce-based compound when observed in *ac* plane, whereas they appear to be more aligned along *b* axis in terms of up or down orientations. The existence of similar crystal structure types is probably related to the preference of the larger rare-earth cations such as Ce^{3+} for a higher average coordination number relative to the smaller Ln^{3+} entities. This feature is not unique, and similar symmetry changes are also observed between $La_2Mo_4O_{15}$ ($P2_1/n$, V = 1228.14 Å^3)[12] and $Ce_2Mo_4O_{15}$ ($P\bar{1}$, V = 1671.37 Å^3)[13] nor La_2MoO_6 ($I4_1/acd$, V = = 1076.56 Å^3)[14] and Tb_2MoO_6 ($C2/c$, V = 935.85 Å^3).[14] In each example, the replacement of lanthanide by lanthanum induced a stronger disorder, which could be at the origin of the change of the unit cell.

The title compound is also isoformular with compounds $Eu_6(Mo_2O_7)(MoO_4)_8$[13] and $Nd_6(Mo_2O_7)(MoO_4)_8$[15] [both crystallized in monoclinic cells, space group $C2/c$ with the parameters a = 12.425(1), b = 19.860(2) and c = 13.882(1) Å, β = 100.767(2)°

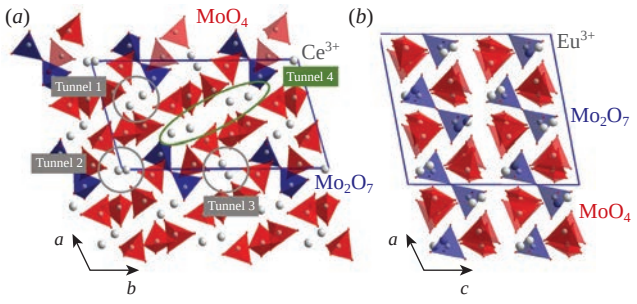

Figure 2 Projections of the crystal structure of (*a*) $Ce_6(Mo_2O_7)(MoO_4)_8$ along *b* axis; three single tunnels 1, 2 and 3 and double tunnel 4 are highlighted; (*b*) $Eu_6(Mo_2O_7)(MoO_4)_8$ showing the absence of tunnels.

and $V = 3269.77(22)$ Å^3 for the Eu compound and $a = 12.3008(5)$, $b = 19.6596(9)$ and $c = 13.7691(4)$ Å, $\beta = 100.8930(9)°$ and $V = 3365.22(50)$ Å^3 for the Nd compound]. Although the local coordination of molybdenum is the same in the three structures with isolated orthomolybdate and one pyromolybdate, the environments of rare-earth cations vary, leading to totally different structures[15] because the molybdenum units do not form La-hosting tunnels.

The complexity calculation using the ToposPro[16] software indicates that our La-based compound ($I_G = 6.78$ bits per atom, $I_{G,\text{total}} = 1492.90$ bits per cell) is more complex than the Ce-based homologue ($I_G = 5.78$ bits per atom, $I_{G,\text{total}} = 635.95$ bits per cell). This value is strongly related to the atomic arrangement of the unit cell using a definition explained.[17] The higher complexity of the La phase compared to the Ce phase agrees quite well with their unit cell parameters and volumes. Because of its high I_G total value, $La_6(Mo_2O_7)(MoO_4)_8$ is defined as a very complex structure, which is rather rare because only 0.02% of inorganic structures are identified as very complex.[17] Here, this value is due to the chemical composition of the unit cell and the number of isolated units (La^{3+}, MoO_4 and Mo_2O_7). Of course, all of this relates to the rather big unit cell volume [$V = 6996.10(42)$ Å^3].

For the moment, our attempts to synthesize a pure powder sample of $La_6(Mo_2O_7)(MoO_4)_8$ from La_2O_3 and MoO_3 mixtures in sealed/open silica tubes or alumina crucibles systematically failed perhaps because of the complexity of the La_2O_3–MoO_3 binary system. The target phase is not observed even in X-ray diffraction patterns. This phase is probably a metastable one difficult to isolate at a scale of a powder sample.

This new lanthanum oxide appears as a potential phosphor capable of hosting Ln^{3+} activators (Eu^{3+}, Sm^{3+}, Ho^{3+}, Er^{3+} *etc*.) towards efficient red and infrared emissions.

This study was supported by the Fonds Européen de Développement Régional (FEDER), CNRS, Région Nord Pas-de-Calais. We are grateful to Ministère de l'Education Nationale de l'Enseignement Supérieur et de la Recherche for funding the X-ray diffractometers and to F. Goutenoire for fruitful discussions.

Online Supplementary Materials

Supplementary data associated with this article can be found in the online version at doi: 10.1016/j.mencom.2017.11.018.

References

1 P. Lacorre, F. Goutenoire, O. Bohnke, R. Retoux and Y. Laligant, *Nature*, 2000, **404**, 856.
2 S. Georges, F. Goutenoire, F. Altorfer, D. Sheptyakov, F. Fauth, E. Suard and P. Lacorre, *Solid State Ionics*, 2003, **161**, 231.
3 G. Corbel, Y. Laligant, F. Goutenoire, E. Suard and P. Lacorre, *Chem. Mater.*, 2005, **17**, 4678.
4 A. Arulraj, F. Goutenoire, M. Tabellout, O. Bohnke and P. Lacorre, *Chem. Mater.*, 2002, **14**, 2492.
5 D. E. Bugaris and H.-C. zur Loye, *Angew. Chem. Int. Ed.*, 2012, **51**, 3780.
6 A. J. Cortese, D. Abeysinghe, B. Wilkins, M. D. Smith, V. Rassolov and H.-C. zur Loye, *Cryst. Growth Des.*, 2016, **16**, 4225.
7 B. M. Gatehouse and R. Same, *J. Solid State Chem.*, 1978, **25**, 115.
8 *SAINT: Area-Detector Integration Software*, Siemens Industrial Automation, Inc., Madison, WI, 1996.
9 G. M. Sheldrick, *SADABS 2.10*, Bruker AXS, Inc., Madison, Wisconsin, USA, 1996.
10 L. Palatinus and G. Chapuis, *J. Appl. Crystallogr.*, 2007, **40**, 786.
11 V. Petříček, M. Dušek and L. Palatinus, *Z. Kristallogr.*, 2014, **229**, 345.
12 F. Dubois, F. Goutenoire, Y. Laligant, E. Suard and P. Lacorre, *J. Solid State Chem.*, 2001, **159**, 228.
13 H. Naruke and T. Yamase, *J. Solid State Chem.*, 2001, **161**, 85.
14 J. S. Xue, M. R. Antonio, and L. Soderholm, *Chem. Mater.*, 1995, **7**, 333.
15 R. S. Barker and I. R. Evans, *J. Solid State Chem.*, 2006, **179**, 1918.
16 V. A. Blatov, A. P. Shevchenko and D. M. Proserpio, *Cryst. Growth Des.*, 2014, **14**, 3576.
17 S. V. Krivovichev, *Angew. Chem. Int. Ed.*, 2014, **53**, 654.

Received: 17th April 2017; Com. 17/5225